Ibn Al-Haitham Journal for Pure and Applied Sciences
Journal homepage: jih.uobaghdad.edu.iq
PISSN: 1609-4042, EISSN: 2521-3407
IHJPAS. 2025, 38(2)

Green Synthesis and Characterization of Vanadium Oxide Nanoparticles using Plant Extract

Saba H. Mahdi[1], Lekaa K. Abdul karem[2*], and Ahmed M. Khalil[3]
[1,2]Department of Chemistry, College of Education for Pure Science (Ibn Al-Haitham), University of Baghdad, Baghdad, Iraq.
[3]Photochemistry Department, National Research Centre, 33 El-Bohouth St, Dokki, Giza, 12622, Egypt
*Corresponding Author.

Received: 25 September 2023 Accepted: 27 December 2023 Published: 20 April 2025
doi.org/10.30526/38.2.3762

Abstract

This study employed the biosynthetic technique for creating vanadium nanoparticles (VNPs), which are affordable and user-friendly; VNPs was synthesized using vanadium sulfate ($VOSO_4.H_2O$) and a plant extract derived from *Fumaria Strumii Opiz* (E2) at a NaOH concentration of 0.1 M. This study aims to investigate the potential applications of utilizing an adsorbent for metal ions to achieve environmentally friendly production and assess its antibacterial activity and cytotoxicity. The reaction was conducted in an alkaline environment with a pH range of 8–12. The resulting product was subjected to various characterization techniques, including Fourier transform infrared spectroscopy, ultraviolet-visible spectroscopy, x-ray diffraction (XRD), transmission- and scanning- electron microscopy (TEM, SEM). The measurement of crystal size in NPs was conducted using Debye Scherer's equation in x-ray diffraction, resulting in a value of 16.06 nm. On the other hand, in the same direction, the size of VO_2 NPs was determined through SEM and TEM. Also, this work investigates the antibacterial properties of VO_2 nanoparticles against four bacterial strains, comprising two gram-positive-negative types and one fungus strain, to evaluate its antifungal efficacy. Notably, the application of newly produced VNPs has demonstrated a significant potential for anticancer activity in cell lines. The SW480 cell line was subjected to MTT assay at various concentrations. The results suggested a positive correlation between concentration and percentage of inhibition. By calculating the IC50 value, which was determined to be 60.3 mg/mL, it can be inferred that this NPs holds potential for targeted therapy in colon cancer treatment. Also, the present study investigates the antibacterial activity of VNPs synthesized using a biosynthetic approach. The cell line SW480 was utilized to evaluate the efficacy of the synthesized VNPs; XRD was employed to analyze the structural properties of the synthesized material.

Keywords: MTT assay, Scanning electron microscopy, Transmission electron microscopy, Vanadium nanoparticles, X-ray diffraction.

1. Introduction

Nanotechnology is the deliberate manipulation of structures, electronics, and systems at the nanometer scale, encompassing dimensions ranging from 1 nm to 100 nm (10^{-9} m) (1,2). The term "nanometer" derives its prefix "Nano" from the Greek word "Nano," denoting "extremely small." The smaller dimensions of these entities afford them a more excellent ratio of surface area to volume compared to their larger counterparts, resulting in enhanced reactivity and the ability to manipulate several attributes (3-5). The unique characteristics of nanoparticles (NPs) have contributed to the advancement of Nanoscience and the utilization of NPs in several domains, such as biomedicine, cosmetics, electronics, food analysis, environmental remediation, and paints (6- 8). The field of Nanoscale science and engineering offers researchers a heightened comprehension and manipulation of materials at the atomic and molecular scales (9). Nanoscale particles' exceptional electrical, optical, and magnetic capabilities have garnered significant interest in recent years (10). NPs are divided into different classes according to their morphology, size, and chemical characteristics (11). This classification system is based on physical and chemical characteristics. Engineered metal oxide NPs (MONPs) are extensively utilized in produced nanomaterials due to their distinct characteristics (12). Numerous NPs exist that hold significant importance within the realm of scientific research. These include gold, copper, iron, zinc, and vanadium dioxide NPs (13). The vanadium, possessing diverse oxidation states, has extensive utility in various chemical, physical, and biological contexts (14). The prevalent types of vanadium oxides include V_2O_5, VO_2, V_2O_3, and VO. Vanadium dioxide finds application in electrical and optical devices (15). Recently, there has been a growing interest in synthesizing vanadium oxide NPs (VNPs) owing to their unique features. In addition to their uses in electrical and optical systems, VNPs remove utilized organic or inorganic pollutants from water (16). In addition, it has been observed that VNPs exhibit cytotoxic effects on both fibroblast and tumor cells (17), induce mitochondrial damage and apoptosis, and possess antimicrobial properties (18). *Fumaria Strumii Opiz* is a well-known species within the Fumariaceae family. The plant is distributed widely across several continents, including Europe, Asia, and Africa (19). It has been documented many therapeutic properties in Bulgarian traditional medicine, including its use as an antihypertensive, heap to protective, and for managing skin rashes (20, 21). F. S. O. is rich in isoquinoline alkaloids and flavone hetero-sides. Protopine, aporphine, benzophenanthridine, and protoberberine are the important alkaloids in *F. Strumii Opiz* (22, 23). The latest study developed a novel method for synthesizing VO_2 using *F. Strumii Opiz*. The technique mentioned earlier was employed in the conducted research. This study aims to investigate the potential applications of utilizing an adsorbent for metal ions to achieve environmentally friendly production and assess its antibacterial activity and cytotoxicity.

2. Materials and Methods

The natural material (E2) was sourced from local origins and then gathered and classified. Sodium hydroxide (NaOH) is utilized as a chemical reagent sourced from Alpha India's Alpha Chemica, while vanadium sulfate hydrate ($VOSO_4$) is employed in many applications. The H_2O was obtained from England. Ethanol is derived from the plant species Sigma Aldrich. Various spectroscopic and microscopic methods were employed to characterize and identify all the compounds. These methods included using a Magnetic Stirrer, a Centrifuge of the PLC type, and an Electric Oven of the Faithful model WHL. 25AB, a Sensitive Electronic Balance of the RADWAG model AS 220C1, a Shaking Water Bath of the SCL FINETEDI kind, pH tapes, UV-Vis measurement using the Shimadzu model (160/UV), FTIR

spectroscopy using the 8500s model, X-ray diffraction (XRD) using the PW1730 type (Phillips/ Holland), FESEM with the MIRAI model, and TEM with the model number EM10C-100 Kv. The intensity of the resulting color was measured using a microplate reader model DNM-9602G after adding MTT dye.

2.1. Preparing of E2 extract

A thorough rinsing with tap water was followed to remove any residual impurities; fresh herbs were then dried after extraction from the water and let air dry for the night. Subsequently, the material was pulverized to facilitate the extraction procedure. After adding 20 grams (g) of the herbs to 200 milliliters (mLs) of deionized water, the resulting mixture was subjected to continuous stirring using a magnetic stirrer for 30 minutes while maintaining a temperature range of 60-70 ºC. Subsequently, the mixture was allowed to cool down to room temperature before being disposed of. The filtration process took place within the centrifuge apparatus. The collected cells were stored in test tubes and centrifuged at 4000 revolutions per minute. This centrifugation step aimed to eliminate residual debris and fibers while preserving the filter's integrity, as shown in **Figure 1** (24).

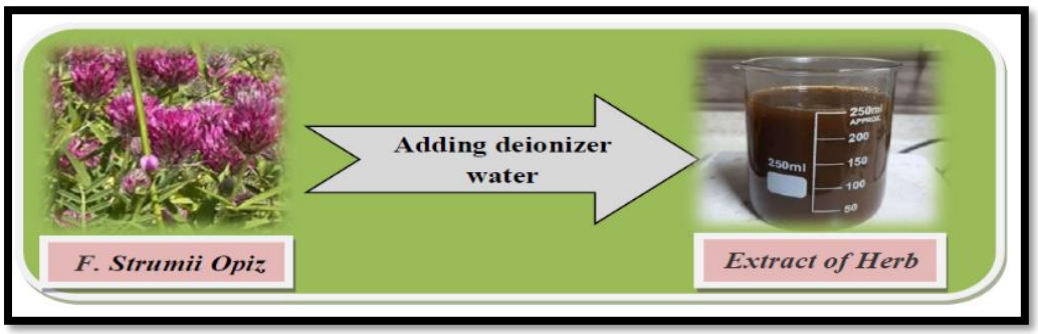

Figure 1. The preparation of E2 extract.

2.2. Preparation of vanadium oxide nanoparticles (VO_2 NPs)

The VO_2 NPs were synthesized utilizing an environmentally benign approach. Following a stirring period of 30 minutes, a volume of 100 mLs of filtered plant extract solution was introduced to an equal volume of aqueous $VOSO_4$ solution. The latter solution was characterized by a concentration of 1.63 g per 100 mLs. Subsequently, 50 mLs of NaOH solution containing 2 g of the compound was gradually added until the pH level reached 12. Upon the elapse of a 60-minute duration at a temperature of 70 ºC, an alteration in coloration was perceived concurrent with precipitation. Following an overnight period of being left undisturbed, the substance was subjected to separation using a centrifuge. Subsequently, it undergoes several rinses with deionized water and was subsequently subjected to drying in an electric oven at a temperature of 300 ºC for 3 hours, as shown in **Figure 2** (25).

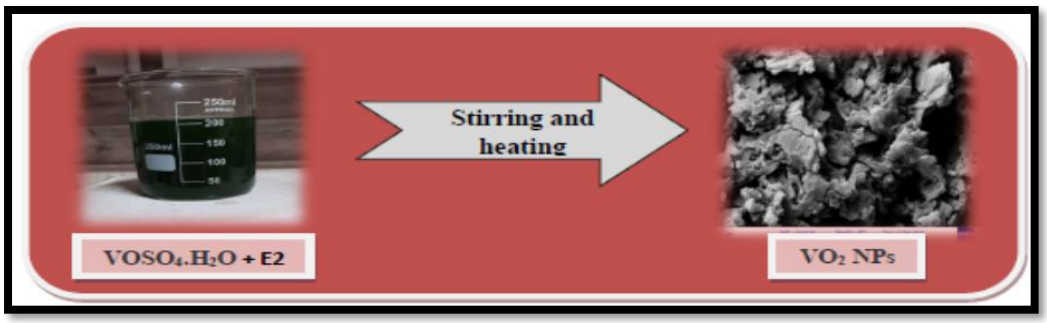

Figure 2. The preparation of VO_2 NPs.

2.3. Biological activity

The bactericidal action of manufactured VO_2 NPs was tested using *Staphylococcus aureus* and *Streptococcus pneumoniae*, both gram-positive bacteria, and *Proteus mirabilis* and *Escherichia coli*, both gram-negative bacteria. This testing was conducted in a nutritional medium known as Muller Hinton agar. The method above was also used to assess the *Candida* fungus's antifungal properties (26).

2.4. Cytotoxic assays

The study utilized the MTT assay to analyze the effectiveness of VNPs on colon cancer cells and determine the extent to which these NPs decrease cellular activity. Then, the calorimetric approach was applied to assess the cells' metabolic activity.

3. Results and Discussion

3.1. The FT-IR spectrum analysis

The infrared spectrum of VO_2 NPs prepared from E2 is shown in **Figure 3** a group of bands that belong to VO_2; the peaks at (678 and 640) cm^{-1} were assigned to terminal oxygen bonds, while the other stretching vibrations at (513, 455, and 412) cm^{-1} were due to V-O bonds. The peaks at (3429, 3182) cm^{-1} referred to OH and C-H aromatic functional groups; it may be due to the remains of organic materials in the extract, respectively (27), while the other peaks are due to the stretching vibrations of the aliphatic C-H bond and the C-C bond.

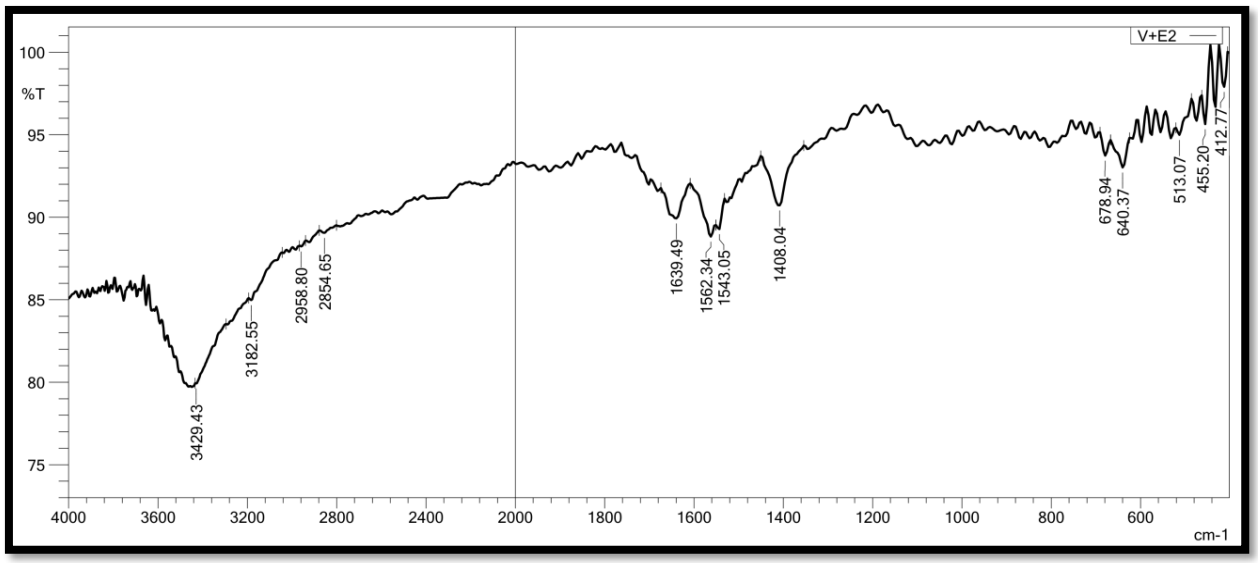

Figure 3. The FTIR of VO_2 NPs.

3.2. The UV-Visible spectrum

The optical properties of the nanoparticles prepared from plant extract and V were verified by ultraviolet-visible spectroscopy. UV-visible is an electromagnetic wave with a wavelength shorter than light. Visible rays are more extended than X-rays, so they are called ultraviolet because the wavelength of the violet color is the shortest between the colors of the spectrum; the wavelengths are covered in the range of 10-400 nm, and energies range from 3 to 124 eV (28). The ultraviolet spectrum of VO_2, which was prepared from E_2, exposed the absorption peak of the transition holes between V and oxygen (O) at 346 nm, as listed in **Figure 4**.

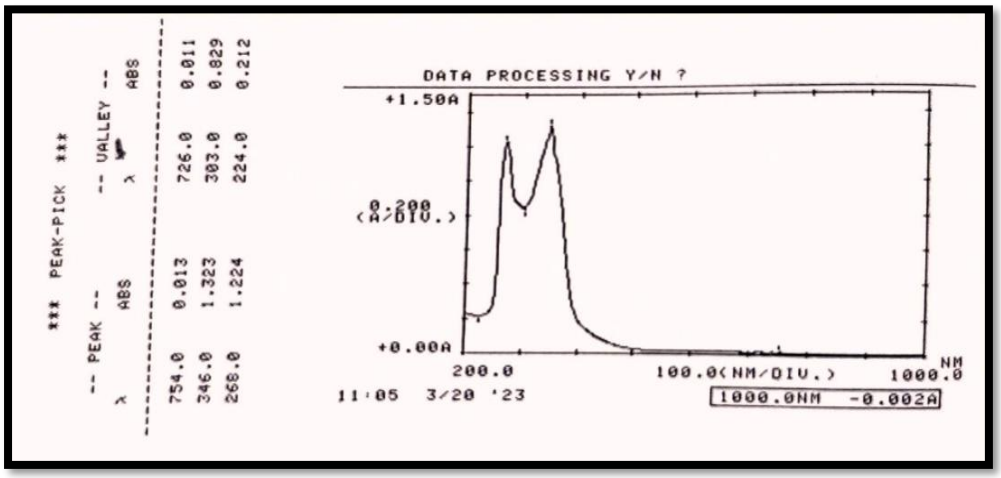

Figure 4. The UV-Vis spectrum of VO_2 NPs.

3.3. The X-Ray diffraction (XRD)

Figure 5 displays an XRD spectroscopic image capturing the as-grown products. The separate peaks of the diffraction pattern exhibited a very narrow breadth at half height. The diffraction patterns of VO_2 NPs were observed at specific angles, namely 18.64°, 25.50°, 28.3°, 30.6°, 37.61°, 40.75°, 54.67, 57.4°, 63.89°, and 67.61^o. These angles correspond to the diffractive crystal planes of -201, 110, 002, -401, 401, 112, 113, and 711, respectively. These observations align with the standard diffraction peaks of VO_2 (JCPDS Card No. 65-7960) (29, 30). Notably, the peaks closely resemble the diffraction pattern observed for VO_2. The evidence unequivocally demonstrates that the products exhibited a monoclinic crystalline structure. The average size of a crystal was determined to be 16.66 nm using the Debye-Scherer equation, which is available in **Table 1**.

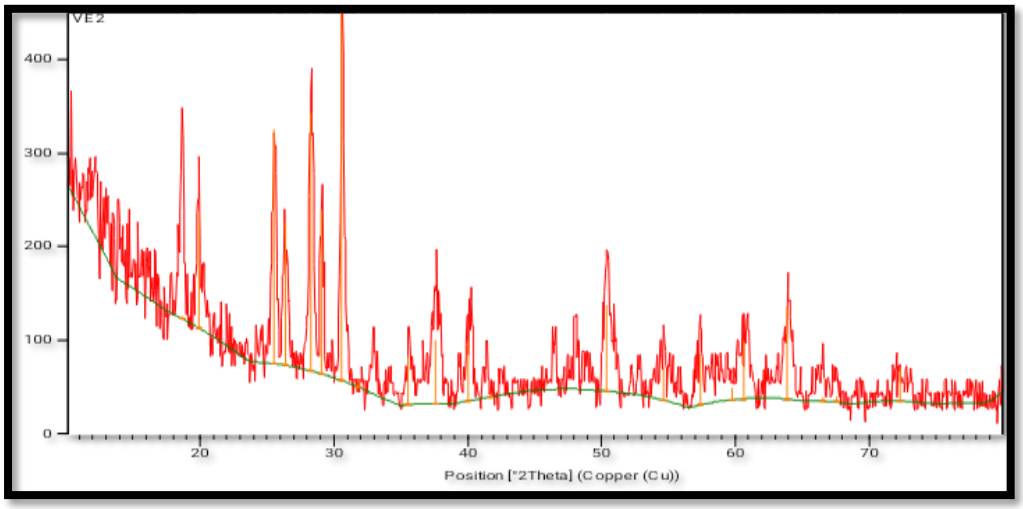

Figure 5. The XRD of VE2 NPs.

3.4. Energy-dispersive X-ray (EDX)

Figure 6 presents the energy-dispersive X-ray (EDX) spectrum of VO_2 NPs, indicating the presence of V and O elements. The spectrum displays distinct peaks that are explicitly linked to various components. The results support the assertion that the synthesized NPs demonstrate significant purity. Moreover, the estimates obtained from the EDX experiment exhibit consistency with the theoretical calculations about elemental composition (31).

Table 1. The data of XRD for VE2 NPs.

Pos. [2θ]	Height [cts]	FWHM [2θ]	Dp (nm)	Dp Average (nm)
18.64	2.59	4.00	2.10	
25.50	250.45	0.3560	23.91	
28. 3	276.42	0.3553	24.10	
30. 6	398.18	0.1977	43.54	
37.61	67.37	1.1163	7.86	
40.75	3.14	0.9199	9.61	16.06
54.67	34.97	1.9094	4.90	
57.4	53.99	0.7075	13.38	
63.9	98.19	0.6624	14.77	
67.61	5.54	1.6725	5.98	

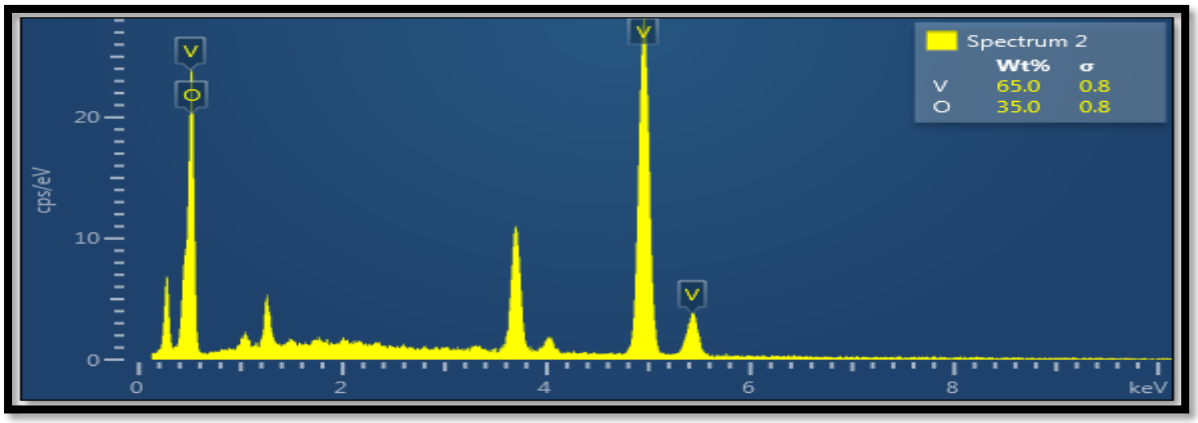

Figure 6. The EDX of VO_2 NPs.

3.5. Field emission scanning electron microscopy (FE-SEM)

Field emission scanning electron microscopy (FE-SEM) is an advanced method to acquire microstructural images of various materials. The accuracy of the creation of VNPs using the E2 extract is confirmed by the observed morphologies of the SEM images and the range of grain diameters, which fall between (13.4-65.22) nm, as shown in **Figure 7** (32, 33).

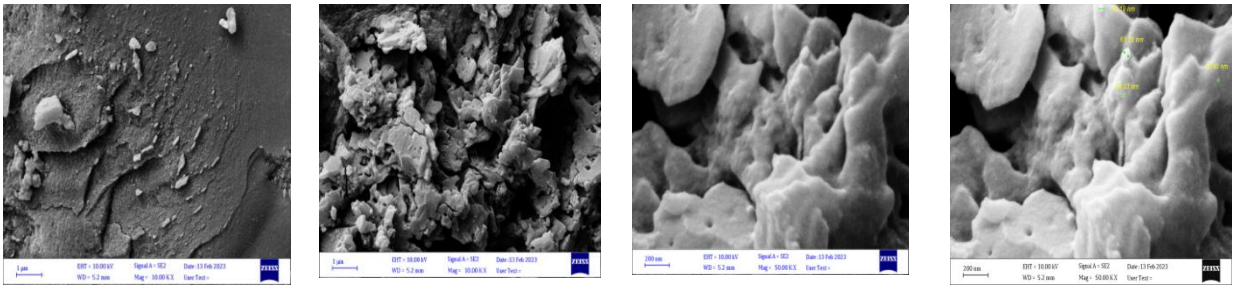

Figure 7. The SEM Images of VO_2 NPs.

3.6. Transmission electron microscopy (TEM)

The shape of VO_2 NPs was found to be aggregated based on the TEM images presented in **Figure 8**. The limited precision of the measurements hinders the estimation of the sample's form. Nevertheless, the sample exhibits zero-dimensional measurements of the spherical structure, with all dimensions falling inside the nanoscale range. This characteristic is greatly favored in surface chemistry for nanomaterials (34).

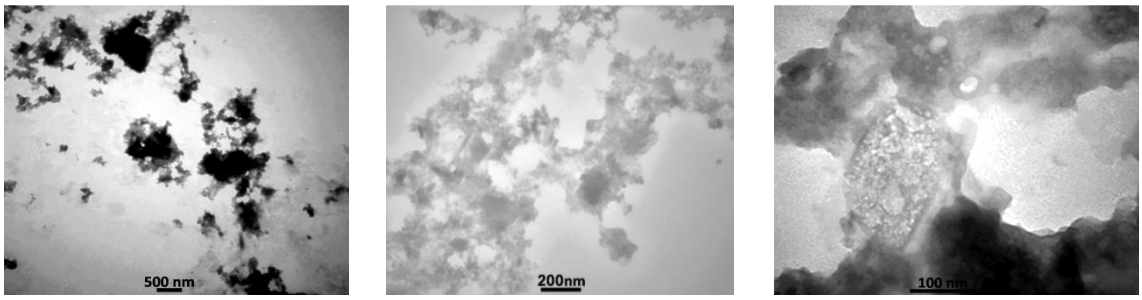

Figure 8. The TEM images of VO_2 NPs.

3.7. Antimicrobial studies

A study on the antibacterial properties of VO_2 NPs was assessed against a total of four bacterial strains (gram-positive: *Staphylococcus aureus*, *Streptococcus pneumoniae*), two gram-negative strains (*Proteus mirabilis, Escherichia coli*), and one fungal strain (Candida) using the healthy plate method on nutritional agar (35, 36). The measurement of the biological activity of the Nano oxide was conducted in millimeters (mm) by assessing the diameter of the inhibition zone (ZI) surrounding each aperture (37). The agar-well diffusion method was employed to investigate the impact of the studied chemical compounds on the organism's growth. This was achieved by adding 20–25 mLs of nutrient agar medium into each petri dish. The experimental results indicate that the produced nano oxide has a significantly higher efficacy against the Candida fungus and *E.coli* than the herb. Simultaneously, a disparity exists in the effectiveness of the VO_2 NPs and the herb against the four distinct bacterial strains, as demonstrated in **Table 2**, **Figures 9** and **10**.

Table 2. The antimicrobial activity of VO_2 NPs.

Compound	*Staphylococcus aureus*	*Streptococcus pneumoniae*	*Escharia coli*	*Proteus mirabilis*	*Candida albicans*
DMSO	___	___	___	___	___
E2	18	22	24	22	20
VO_2	21	21	23	21	23

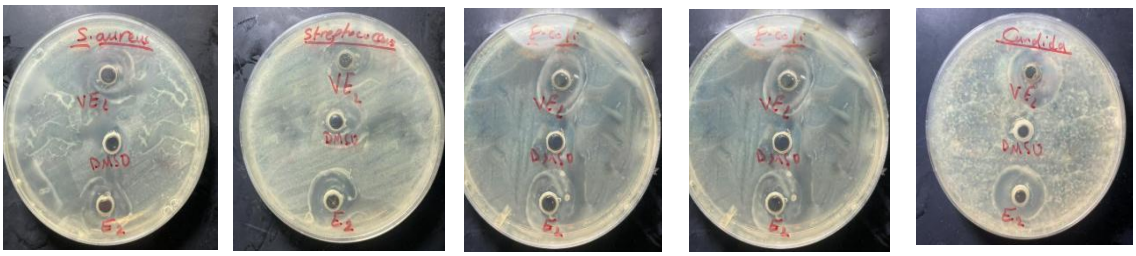

Figure 9. Zone of growth inhibition against bacteria' series and fungi.

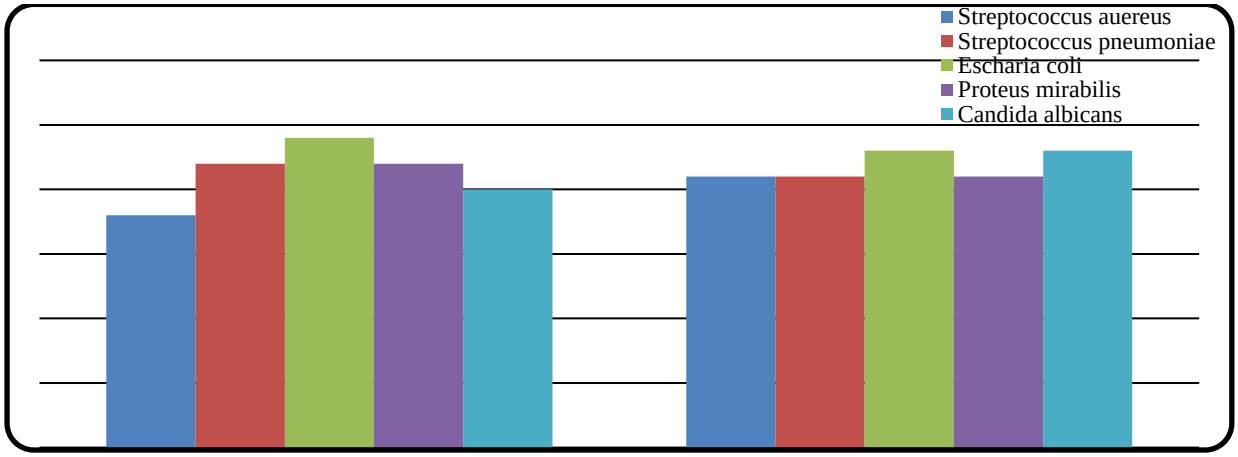

Figure 10. The (ZI) mm of VE2 NPs.

3.8. The assessment of cell viability and cytotoxicity using MTT assays

The experimental approach employed in this study utilized the SW480 cancer cell line. The dye known as 3-(4,5-dimethylthiazol-2-yl)-2,5-diphenyl tetrazolium bromide (MTT), which possesses a discernible color, is employed to assess cellular viability (38, 39). The findings of this study indicate that V oxides exhibited a pronounced cytotoxicity towards cancer cells. The subsequent sections will provide a comprehensive explanation of this topic. This study aimed to assess the magnitude of the harmful impact by determining the percentage of growth inhibition rate (referred to as the Inhibition Rate) over 24 hours at a temperature of 37°C. The experimental results indicate that the cell viability percentage was the lowest (10.09%) when the cell line colon cancer was treated with the produced NPs at a concentration of 500 µg/mL. This corresponds to the highest inhibition percentage, as presented in **Table 3**. The findings indicate that the concentration of the substance employed is crucial in determining the degree of cell inhibition. The study revealed that an elevated concentration level leads to a decrease in the viability percentage, which increases the inhibition percentage of cell growth in the malignant cell line (40). This relationship is visually represented in **Table 3** and **Figure 11**. Significantly, the observed magnitude of the resultant hue is at a specific wavelength of 570 nm.

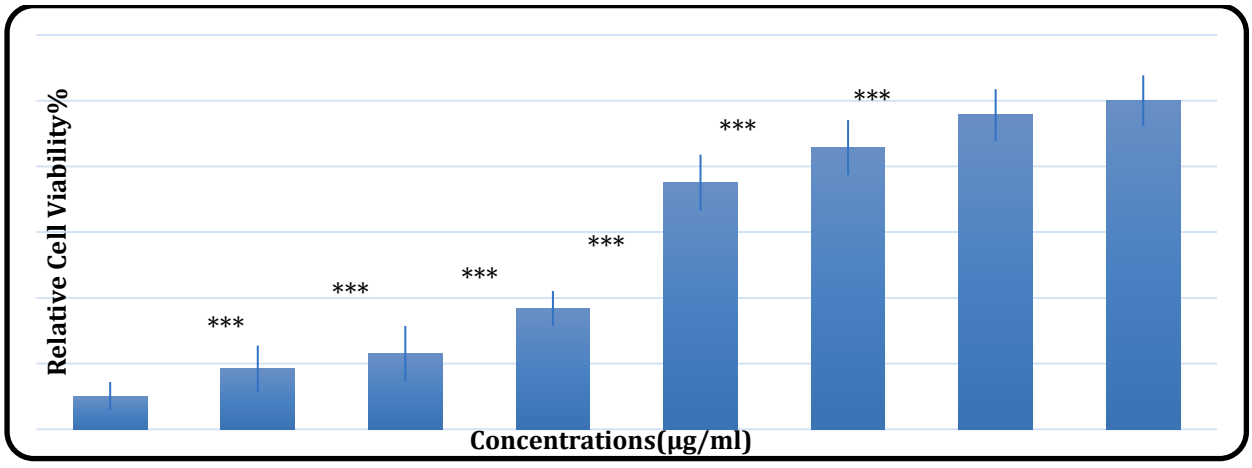

Figure 11. The percentage of viability in the cells of the cancer line SW480 of VO_2 NPs.

Table 3. Statistical values of SW480 colon cancer cell line of VO_2 NPs.

Concentration mg/ml	Relative Cell Viability %	Number of Values	Standard deviation
7.81	95.64	8	0.027
15.625	85.72	8	0.024
31.25	75.07	8	0.026
62.5	36.80	8	0.030
125	23.06	8	0.028
250	18.39	8	0.025
500	10.09	8	0.021

3.9. The IC50 of VO_2 NPs

One of the most significant findings from the conducted tests on VO_2 NPs and their effect on the SW480 cancer cell line is the determination of the half-inhibition concentration (IC50) (41,42). This concentration, represented by IC50, was at which approximately 50% of the cells were killed. The interaction with NPs and a colon cancer cell line was investigated, revealing a half-inhibitory dose of 60.3µg/mL. This auspicious outcome indicates that VNPs derived from *F. Strumii Opiz* extract could effectively eliminate colon cancer cells. The results of this study hold considerable importance in the use of selective treatment for colon cancer, as illustrated in **Figures 12** and **13**.

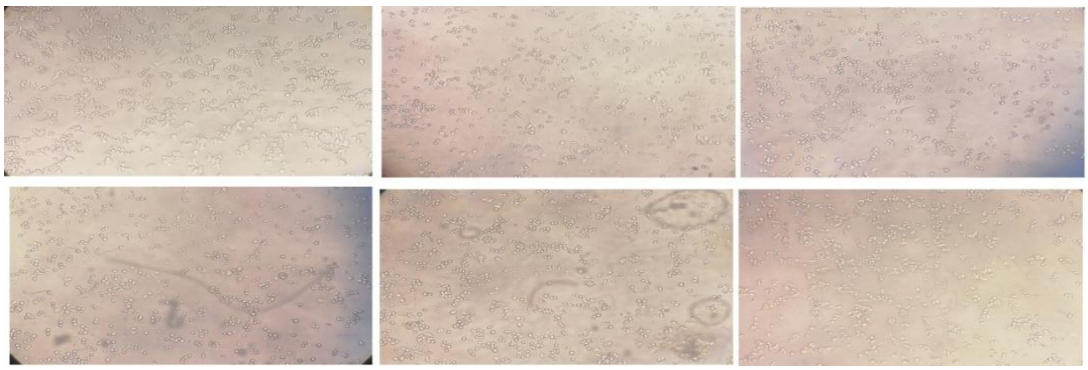

Figure 12 . Cancer cells treated with VO_2 NPs at different concentrations after addition.

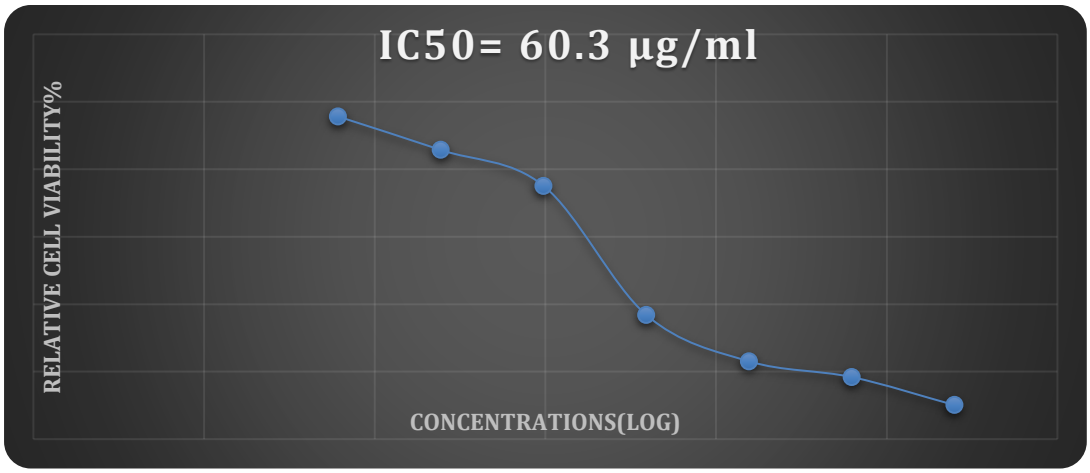

Figure 13. The half Inhibition Fifty (IC_{50}) of VO_2 NPs.

4. Conclusion

The synthesis of vanadium oxide NPs was carried out using a sustainable method, which involved the utilization of *Fumaria Strumii Opiz* extract and $VOSO_4.H_2O$. The crystals obtained displayed a monocrystalline structure with a diameter of 16.06 units. The particles demonstrated varying activity levels against four distinct bacterial strains, including two gram-positive strains (*Staphylococcus aureus*, *Streptococcus pneumoniae*) and two gram-negative strains (*Proteus mirabilis*, *Escherichia coli)*. In addition, the particles exhibited significant efficacy against *Candida*, a type of fungus, displaying the utmost activity level. On the other hand, the cytotoxicity of the nano-oxide was evaluated on the SW480 colon cancer cell line, demonstrating an average IC50 cell inhibition of 60.3 mg/mL. The results of this study are of significant importance in the application of targeted therapy for colon cancer.

Acknowledgment

The authors thank the Department of Chemistry, College of Education for Pure Science (Ibn Al-Haitham), University of Baghdad, for generously providing resources to support this research endeavor.

Conflict of Interest

The authors declare that they do not have any competing interests.

Funding

There was no financial source.

Ethical Clearance

The study has been approved by the Committee of the University of Baghdad/ College of Education for Pure Science (Ibn Al-Haitham) and done by the ethical standards set out in 1964

References

1. Farooqi ZU, Qadeer A, Hussain MM, Zeeshan N, Ilic P. Characterization and physicochemical properties of nanomaterials. In Nanomaterials: Synthesis, characterization, hazards and safety. Elsevier; 2021, pp. 97-121. https://dx.doi.org/10.1016/B978-0-12-823823-3.00005-7.

2. Salem SS, Fouda A. Green synthesis of metallic nanoparticles and their prospective biotechnological applications: an overview. Biol Trace Elem Res. 2021; 199(1):344-370. https://doi.org/10.1007/s12011-020-02138-3.

3. Barik TK, Maity GC, Gupta P, Mohan L, Santra TS. Nanomaterials: an introduction. In book: Nanomaterials and their biomedical applications. 2021, p.1-27. https://doi.org/10.1007/978-981-33-6252-9_1.

4. Singh BK, Lee S, Na K. An overview on metal-related catalysts: Metal oxides, nanoporous metals and supported metal nanoparticles on metal organic frameworks and zeolites. Rare Metals. 2020; 39:751-766. https://doi.org/10.1007/s12598-019-01205-6.

5. Salem SS, Fouda MM, Fouda A, Awad MA, Al-Olayan EM, Allam AA, Shaheen TI. Antibacterial, cytotoxicity and larvicidal activity of green synthesized selenium nanoparticles using Penicillium corylophilum. J Clust Sci. 2021; 32:351-361. https://doi.org/10.1007/s10876-020-01794-8.

6. Khan S, Mansoor S, Rafi Z, Kumari B, Shoaib A, Saeed M, Alshehri S, Ghoneim MM, Rahamathulla M, Hani U, Shakeel F. A review on nanotechnology: Properties, applications, and mechanistic insights of cellular uptake mechanisms. J Mol Liq. 2022; 348:118008.https://doi.org/10.1016/j.molliq.2021.118008.

7. Pérez-Hernández H, Pérez-Moreno A, Sarabia-Castillo CR, García-Mayagoitia S, Medina-Pérez G, López-Valdez F, Campos-Montiel RG, Jayanta-Kumar P, Fernández-Luqueño F. Ecological drawbacks of nanomaterials produced on an industrial scale: collateral effect on human and environmental health. Water Air Soil Poll. 2021; 232(435):1-33. https://doi.org/10.1007/s11270-021-05370-2.

8. Abd Elkodous M, El-Husseiny HM, El-Sayyad GS, Hashem AH, Doghish AS, Elfadil D, Radwan Y, El-Zeiny HM, Bedair H, Ikhdair OA, Hashim H. Recent advances in waste-recycled nanomaterials for biomedical applications: Waste-to-wealth. NTREV. 2021; 10(1):1662-739. https://doi.org/10.1515/ntrev-2021-0099.

9. Bayda S, Adeel M, Tuccinardi T, Cordani M, Rizzolio F. The history of nanoscience and nanotechnology: From chemical–physical applications to nanomedicine. Molecules. 2019; 25(1):112.

112, https://doi.org/10.3390/molecules25010112.

10. Qiu L, Zhu N, Feng Y, Michaelides EE, Żyła G, Jing D, Zhang X, Norris PM, Markides CN, Mahian O. A review of recent advances in thermophysical properties at the nanoscale: From solid state to colloids. Phys Rep. 2020; 843:1-81.https://doi.org/10.1016/j.physrep .2019.12.001.

11. Hyman P, Denyes J. Bacteriophages in nanotechnology: History and future. In book: Bacteriophages: Biology, technology, therapy. 2021; 657-587. https://doi.org/10.1007/978-3-319-41986-2_22-1.

12. Chavali MS, Nikolova MP. Metal oxide nanoparticles and their applications in nanotechnology. SN Appl Sci. 2019; 1:607. https://doi.org/10.1007/s42452-019-0592-3.

13. Kareem EA, Sultan AE, Oraibi HM. Synthesis and characterization of silver nanoparticles: A review. IHJPAS. 2023; 36(3):177-200. https://jih.uobaghdad.edu.iq/index.php/j/article/view/3050.

14. Wang J, Yuan Q, Morovvati H, Goorani S. Green synthesis, characterization and anti-atherosclerotic properties of vanadium nanoparticles. Inorg Chem Commun.. 2022; 146(9226):110092. https://doi.org/10.1016/j.inoche.2022.110092.

15. Barreto A, Santos J, Amorim MJ, Maria VL. Environmental hazards of boron and vanadium nanoparticles in the terrestrial ecosystem—A case study with enchytraeus crypticus. Nanomaterials. 2021; 11(8):1937. https://doi.org/10.3390/nano11081937.

16. Bueloni B, Sanna D, Garribba E, Castro GR, León IE, Islan GA. Design of nalidixic acid-vanadium complex loaded into chitosan hybrid nanoparticles as smart strategy to inhibit bacterial growth and quorum sensing. Int J Biol Macromol. 2020; 161:1568-80.https://doi.org/10.1016/j.ijbiomac.2020.07.304.

17. Diniz MO, Golin AF, Santos MD, Bianchi RF, Guerra EM. Improving performance of polymer-based ammonia gas sensor using POMA/V2O5 hybrid films. Org Electron. 2019; 67:215-221. https://doi.org/10.1016/j.orgel.2019.01.039.

18. Dadkhah M, Tulliani JM. Green synthesis of metal oxides semiconductors for gas sensing applications. Sensors. 2022; 22(13):4669. https://doi.org/10.3390/s22134669.

19. Ali AT, Karem LK. Biosynthesis, characterization, adsorption and antimicrobial studies of vanadium oxide nanoparticles using punica granatum extract. Baghdad Sci J. 2024; 21(2):0410.

https://doi.org/10.21123/bsj.2023.8114.

20. Huang Y, Zhu C, Xie R, Ni M. Green synthesis of nickel nanoparticles using Fumaria officinalis as a novel chemotherapeutic drug for the treatment of ovarian cancer. J Exp Nanosci. 2021; 16(1):368-381. https://doi.org/10.1080/17458080.2021.1975037.

21. Li C, Zhang Y, Li M, Zhang H, Zhu Z, Xue Y. Fumaria officinalis-assisted synthesis of manganese nanoparticles as an anti-human gastric cancer agent. Arab J Chem. 2021; 14(10):103309. https://doi.org/10.1016/j.arabjc.2021.103309.

22. Adham AN, Naqishbandi AM, Efferth T. Cytotoxicity and apoptosis induction by Fumaria officinalis extracts in leukemia and multiple myeloma cell lines. J Ethnopharmacol. 2021; 266:113458. https://doi.org/10.1016/j.jep.2020.113458.

23. Hamid A, Haq S, Ur Rehman S, Akhter K, Rehman W, Waseem M, Ud Din S, Hafeez M, Khan A, Shah A. Calcination temperature-driven antibacterial and antioxidant activities of fumaria indica mediated copper oxide nanoparticles: Characterization. Chem Pap. 2021; 75(20):4189-4198. https://doi.org/10.1007/s11696-021-01650-7.

24. Ghani S, Rafiee B, Bahrami S, Mokhtari A, Aghamiri S, Yarian F. Green synthesis of silver nanoparticles using the plant extracts of vitex agnus castus L: An ecofriendly approach to overcome antibiotic resistance. Int J Prev Med. 2022;13:133. https://doi.org/10.4103/ijpvm.ijpvm_140_22.

25. Al Jabbar JL, Apriandanu DO, Yulizar Y, Sudirman S. Synthesis, characterisation and catalytic activity of V2O5 nanoparticles using Foeniculum vulgare stem extract. In IOP Conference Series: MSE. 2020; 763(1):012031. https://doi.org/10.1088/1757-899X/763/1/012031.

26. Amer AA. Biological evaluation and antioxidant studies of NiO, PdO and Pt nanoparticles synthesized from a new Schiff base complexes. IHJPAS. 2022; 35(4):170-182. https://doi.org/10.30526/35.4.2864.

27. Mahdi SH, Karem LA. Synthesis, spectral and biochemical studies of new complexes of mixed ligand Schiff base and anthranilic acid. Orient J Chem. 2018; 34(3):1565-172. http://dx.doi.org/10.13005/ojc/340349.

28. Abeed BS, Al-Shmgani HS, Khalil KA, Mohammed HA. Evaluation of the potential protective role of galangin associated with gold nanoparticles in the histological and functional structure of kidneys of adult male albino mice Mus musculus administration with carbon tetrachloride. IHJPAS. 2023; 36(3):72-84. https://doi.org/10.30526/36.3.3250.

29. Zhang Y, Tan X, Meng C. The influence of VO (B) nanobelts on thermal decomposition of ammonium perchlorate. Mater Sci-Pol. 2015; 33(3):560-565. http//: 10.1515/msp-2015-0080.

30. Afify HH, Hassan SA, Obaida M, Abouelsayed A. Influence of annealing on the optical properties of monoclinic vanadium oxide VO_2 prepared in nanoscale by hydrothermal technique. Physica E Low Dimens Syst Nanostruct. 2019; 114:113610. https:// doi.org /10. 1016 /j.physe.2019.113610.

31. Subramanian M, Dhayabaran VV, Shanmugavadivel M. Room temperature fiber optic gas sensor technology based on nanocrystalline $Ba_3(VO_4)_2$: Design, spectral and surface science. Mate Res Bull. 2019; 119:110560. https://doi.org/10.1016/ j. materresbull . 2019.110560.

32. Jaya RP. Porous concrete pavement containing nanosilica from black rice husk ash. In New Materials in Civil Engineering 2020; pp. 493-527. https: //doi.org/ 10.1016 /B978-0-12-818961-0.00014-4.

33. Al-Bahadili ZR, Al-Hamdani AA, Rashid FA, Al-Zubaidi LA, Ibrahim SM. An evaluation of the activity of prepared zinc nanoparticles with extracted alfalfa plant in the treatment of heavy metals. Baghdad Sci J. 2022; 19(6):1399. https://dx.doi.org/10.21123/bsj.2022.

34. Saad FA, El-Ghamry HA, Kassem MA, Khedr AM. Nano-synthesis, Biological Efficiency and DNA binding affinity of new homo-binuclear metal complexes with sulfa azo dye based ligand for further pharmaceutical applications. J Inorg Organomet Polym Mater. 2019; 29: 1337-1348. https://doi.org/10.1007/s10904-019-01098-z.

35. Abdalsahib NM, Karem LK. Preparation, characterization, antioxidant and antibacterial studies of new metal (ii) complexes with Schiff base for 3-amino-1-phenyl-2-pyrazoline-5-one. IJDDT. 2023;13(1): 290-296. https://doi.org/10.25258/ijddt.13. 2.33.

36. Mahdi SH, Karem LK. Synthesis, physicochemical studies and biological estimation of new mixed ligand complexes from hetrocyclic compounds. IJPR. 2020; 2(1):1734-1740.

https://doi.org/10.31838/ijpr/2020.SP1.267.

37. Alsahib SA. Characterization and biological activity of some new derivatives derived from sulfamethoxazole compound. Baghdad Sci J. 2020; 17(2):471-480.

http://dx.doi.org/10.21123/ bsj.2020.17.2.0471.

38. Mohan B, Shaalan N. Synthesis, spectroscopic, and biological activity study for new complexes of some metal ions with Schiff bases derived from 2-hydroxy naphthaldehyde with 2-amine benzhydrazide. IHJPAS. 2023; 36(1):208-224. http://doi.org/10.30526/36.1.2978.

39. Baqer SR, Alsammarraie A, Alias M, Al-Halbosiy M, Sadiq A. In vitro cytotoxicity study of pt nanoparticles decorated TiO_2 nanotube array. Baghdad Sci J. 2020; 17(4):1169.

https://doi.org/10.21123/bsj.2020.17.4.1169.

40. Naji SH, Karim LK, Mousa FH. Synthesis, spectroscopic and biological studies of a new some complexes with n-pyridin-2-ylmethyl-benzene-1,2 diamine. IHJPAS. 2013; 26(1):193-207.

41. Abdalsahib, N.M.; Karem, L.K.A. Synthesis, characterization, antioxidant and antibacterial studies for new Schiff base complexes derived from 4-bromo-O-toluiodine. IJDDT. 2023; 13(2):679-685.

http://doi.org/10.25258/ijddt.13.2.33.

42. Carreño EA, Alberto AVP, De Souza CAM, De Mello HL, Henriques-Pons A, Anastacio Alves L. Considerations and technical pitfalls in the employment of the MTT assay to evaluate photosensitizers for photodynamic. Appl Sci. 2021; 11(6):2603. https://doi.org/10.3390/app11062603.